Desalination and Water Treatment
www.deswater.com

doi:10.5004/dwt.2018.22615

120 (2018) 217–227
July

Tailored activated carbons prepared by phosphoric activation of apricot, date and loquat stones and their mixtures; relation between the pore size and the composition in biopolymer

Karima Larbi[a,b], Nouredine Benderdouche[a], Laurence Reinert[b], Jean Marc Lévéque[b], Sandrine Delpeux-Ouldriane[c], Mohamed Benadjemia[a], Benaouda Bestani[a], Laurent Duclaux[b,*]

[a]*Laboratoire de structure, Élaboration et Application des Matériaux Moléculaires (SEA2M), Université Abdelhamid Ibn Badis, Mostaganem, 27000, Algeria*

[b]*Laboratoire de Chimie Moléculaire et Environnement, Université Savoie Mont Blanc, 73000 Chambéry, France, Tel. +33 479758805, email: laurent.duclaux@univ-smb.fr (L. Duclaux)*

[c]*ICMN, CNRS-Université d'Orléans, 45071 Orléans cedex 2 France*

Received 24 December 2017; Accepted 11 June 2018

ABSTRACT

Activated carbons of various physico-chemical characteristics were prepared from singly apricot, loquat or date stones, and from binary mixtures of them (50/50 mass %) by phosphoric acid activation. The content in each of the three biopolymers was quantified by chemical and thermogravimetric analyses. The surface chemistry of the activated carbons was characterized by elemental analysis, Boehm titrations, point of zero charge measurements and infrared spectroscopy, and their porous texture by adsorption of N_2 at 77 K and of CO_2 at 273 K. In the studied conditions of impregnation, precursors bearing high hemicellulose contents, such as loquat stones, have afforded highly mesoporous activated carbons, whereas activated carbons stemming from precursors richer in lignin and cellulose (i.e. apricot and date stones) have been found mainly microporous. The adsorption properties of methylene blue on the prepared activated carbons have been compared and tentatively correlated to their porosity and surface chemistry characteristics.

Keywords: Mesoporous materials; Microporous materials; Activated carbon; Adsorption; Surface chemistry; Porosity, Methylene blue; Phosphoric activation; Biopolymer

1. Introduction

Despite the numerous studies dealing with the purification of wastewater, the topic is still of great concern, as human and industrial activities continually release new polluting molecules in the environment. Many processes, such as flocculation, coagulation, chlorination, ozonation and adsorption, are commonly used with more or less satisfying efficiency to improve water quality [1]. Among the different techniques, adsorption is one of the most widespread methods, due to its low cost and easy implementation [2,3]. Even if a wide range of adsorbents have been developed by the scientific community, this research area is still a burgeoning one with the challenge of finding the most suitable adsorbent for a given adsorbate. Indeed, the efficiency of a depollution process is directly linked to the adsorbent/adsorbate interactions and to the adsorbent's porosity [4,5].

Activated carbons (ACs) are among the most used adsorbents for water quality improvement thanks to their high adsorption efficiencies, especially toward organic pollutants [6]. These adsorbents can be produced by chemical or physical activation of a wide range of precursors [7]. The literature reports the elaboration of ACs by activation of a styrene–divinylbenzene copolymer [8], polyacrylonitrile fibers [9], phenolic resins [10], oil sludge [11] and animal bones [12] etc.

*Corresponding author.

Many ACs have been prepared by phosphoric acid activation of local biomass (wood, straw, cotton stalk, etc.), as this method is easy to perform and can generate, depending on the experimental conditions, high surface area microporous/mesoporous adsorbents [13–17]. One key parameter influencing the development of the porosities of the ACs produced by phosphoric activation is the impregnation ratio [18–20]. As for example, Molina-Sabio and Rodriguez-Reinoso brought out that the activation of lignocellulosic precursors using low phosphoric acid impregnation ratios generated mainly microporous ACs, whereas an additional mesoporosity could be developed by increasing the acid concentration [18]. A second factor influencing the textural characteristics of the adsorbents is the content in biopolymers, such as cellulose, hemicellulose and lignin, which are the main components but in different percentages according to considered biomass precursors [21,22].

Typically, Rodriguez Correa et al. [23] have shown that, by KOH activation of various biopolymers, cellulose afforded ACs of highest surface areas and porous volumes, closely followed by lignin, whereas hemicellulose resulted in lowest surface areas and microporosities.

Jagtoyen and Derbishire [24] reported that the mechanism of phosphoric activation of wood consists in the addition or insertion of phosphate groups in the biopolymer matrix, yielding to a dilation process, resulting after removal of the acid in an expanded state with an accessible pore structure. They also stated that this acidic activation of the amorphous hemicellulose and lignin produced mostly micropores, while the activation of crystalline cellulose afforded materials of wider pore size distributions.

Guo and Rockstraw [25] also reported that the development of porosity was contributory of the preparation conditions (H_3PO_4/precursor impregnation ratio and final activation temperature) and of the nature of the polymeric precursor. According to these authors, hemicellulose, which is the most reactive polymer towards H_3PO_4, developed the greatest mesoporosity at a relatively low impregnation ratio (<1.1) and mild temperatures (<400°C).

Agro-food industry generates large quantities of biomass which constitute interesting precursors of ACs due to their contents in lignocellulosic biopolymers, in particular by-products such as seed hulls, fruit stones, vegetable peels, crustacean shells, etc. The valorization of these natural resources is of great concern as their elimination/disposal represents non-negligible additional operating costs. Over the last two decades, many studies explored the elaboration of low cost materials for specific applications from various by-products [26,27] and particularly from fruit stones. Using sulfuric acid as an activating agent, Mouni et al. have developed an AC of ~400 $m^2 \cdot g^{-1}$ surface area that was tested for Pb(II) adsorption at low concentration [28]. More recently, Marzbali et al. prepared an AC by phosphoric activation of apricot nut shells but their experimental conditions did not allow them to develop specific surface areas (BET) higher than ~300 $m^2 \cdot g^{-1}$ [29]. ACs were also obtained by a one-step physical activation of apricot stones (water vapor, 700°C) by Şentorun-Shalaby et al., yielding to surface areas below 500 $m^2 \cdot g^{-1}$ [30]. Through the physical activation with carbon dioxide, Sekirifa et al. have produced microporous activated carbons of BET specific surface area of about 500 $m^2 \cdot g^{-1}$, possessing high adsorption uptakes of 4-chlorophenol from aqueous solutions [31]. Loquat stones chemically activated by NaOH and KOH [32] have given high specific surface area ACs (1590–2900 $m^2 \cdot g^{-1}$). Very recently, Plaza-Recobert et al. have prepared some super activated carbons by CO_2 activation of loquat stones [33] with very high surface areas reaching 3500 $m^2 \cdot g^{-1}$.

As described above, numerous studies on the elaboration of ACs from one type of fruit waste have already been published. However and up to our knowledge, the AC preparation from mixtures of various fruit wastes has never been described in literature yet.

The aim of this work is to develop low cost ACs by phosphoric acid activation of binary mixtures of apricot, date and loquat stones originating from Algeria. These three lignocellulosic precursors have been selected for their different contents in hemicellulose, cellulose and lignin biopolymers with the aim of producing highly porous adsorbent materials with tailored micro/meso porosities. Another objective was to study the effect of the variation of the biopolymer composition on the porous volume and pore size of the produced activated carbons. Prior to the preparation of the ACs, the selected precursors have been fully characterized and their contents in biopolymers (cellulose/lignin/hemicellulose) determined. The textural properties and surface chemistry of the prepared adsorbents have also been characterized and correlated to their adsorption capacities of methylene blue.

2.Materials and methods

2.1. Biopolymer analyses of the precursors

2.1.1. Thermogravimetric analyses

The thermal decomposition of each precursor was studied on a SETARAM LABSYS TG apparatus, under a N_2 flow (20 $mL \cdot min^{-1}$), with a heating rate of 4°C·min^{-1}. Analyses were performed using about 25 mg of sample.

2.1.2. Chemical extraction of the biopolymers

Prior to the composition study of the different constitutive biopolymers of stones, the extractable organics (resins, fatty acids, oil, grease, etc.) have been removed using ASTM D1107-56 method [34], i.e., by heating and stirring for 8 h under reflux a mixture of 2 g of precursor powder (Apricot, Date or Loquat) in 100 mL of an ethanol-toluene mixture (1:2 vol:vol). After filtration, the solid was dried at 100°C and weighed in order to determine the mass % of the extractable organics.

In a second step, the lignin has been extracted from the dried solid obtained previously (exempt of extractable organics) by using boiling sulfuric acid according to ASTM D1106 – 56 standard method. 1 g of the dried powder was agitated with 15 mL of sulfuric acid (75 mass %) for 2 h at room temperature. Then, 560 mL of water were added and the resulting mixture was let under reflux for 4 h. The solution was then filtered off and the resulting solid was washed with distilled water (500 mL) and dried (100°C). The percentage of lignin was estimated by difference of weight between original and treated samples for each precursor.

In a third step, the holocellulose (i.e. both the cellulose and hemicellulose) was extracted from the dried powder

exempt of extractable organics. 2 g of powder were mixed in a flask with 150 mL of distilled water, 0.2 mL of glacial acetic acid and 1 g of sodium chlorite ($NaClO_2$). The resulting mixture was then heated under reflux and stirred at 80°C for a total duration of 5 h. During this heating period, 1 g of $NaClO_2$ and 0.2 mL of glacial acetic acid were added every hour. The mixture was further cooled in an ice bath and filtrated. The solid was washed with distilled water (500 mL) and dried at 100°C. The percentage of holocellulose was estimated by difference of weight between original and treated samples for each precursor.

For the cellulose content, 3 g of the powder obtained after the third step were poured in 100 mL of a NaOH solution (17.5 mass %) for 30 min. 50 mL of distilled water were then added and the dispersion was stirred for 5 min and filtrated. The solid was washed firstly with a NaOH solution (8.3 mass%; 100 mL), secondly with acetic acid (10 mass%; 40 mL), thirdly with distilled water (1 L), and finally dried (100°C). The percentage of cellulose was estimated by weight difference of between original and treated samples for each precursor.

2.2. Preparation of the activated carbons

ACs were prepared from raw lignocellulosic precursors and from their mixtures. Three precursors originating from Algerian food industry waste have been selected: apricot stones (from Relizane), date stones (from Ghardaia, South Algeria) and loquat stones ("*Eriobotrya japonica*" from Blida). The collected stones from a single variety of fruits and the mixtures of two different stones (50 mass % each) were washed with boiling distilled water to eliminate the dust and the water soluble substances. After drying (105°C, 24 h), they were crushed in a mortar and sieved (<0.071 mm). The sieved powders (samples of 40 g) were impregnated by 200 mL of H_3PO_4 (50 mass%, Sigma-Aldrich) under reflux at 110°C for 3 h. The impregnated powders were then filtered, dried (25°C, 24 h), giving impregnation ratio in the 0.4–1.25 range (defined as the ratio of the weight of H_3PO_4 (g) to the weight of dried precursor (g)) and further heat-treated in air (700°C, 3 h). The temperature of heat treatment of 700°C was chosen instead of 500°C or 600°C in order to optimize the iodine number of the prepared activated carbons. After heat treatment, the activated carbons were extensively washed with distilled water until no phosphate ions were detected in water by a lead nitrate test and further dried (170°C, 3 h). The obtained ACs were sieved to keep particles fractions lower than 0.071 mm. The mass losses due to activation reached 65 to 77%. The six prepared ACs from apricot, date, loquat, apricot/date, apricot/loquat and date/loquat stones have been labeled A, D, L, A/D, A/L and D/L, respectively.

2.3. Physico-chemical characterization of the activated carbons

2.3.1. Chemical analysis

The carbon, hydrogen, oxygen, nitrogen and sulfur weight contents of the precursors and of the ACs were measured using a Thermo scientific CHNS/O – FLASH2000 elemental analyzer (accuracy of ± 0.3%).

The ash contents were determined after heating in an oven under air atmosphere at 650°C for 16 h, according to the ASTMD2866-70 standard method.

The "yield" of the ACs preparation is defined as the ratio of the mass of the AC to the one of the dry stone precursors. The "burn off" is the weight loss percentage due to the activation step.

2.3.2. Characterization of the surface chemistry

The morphology of the samples was observed by scanning electron microscopy (SEM), using a LEO-Stereoscan 440 microscope. Local chemical compositions were determined using a Bruker AXS Quantax EBSD spectrometer coupled to the microscope.

ATR-FTIR measurements were carried out on a Thermo Scientific Nicolet iS10 spectrometer equipped with a germanium crystal. 64 scans were cumulated for each spectrum, with a spectral resolution of 4 cm^{-1}.

The pH_{PZC} (pH of the point of zero charge) of the ACs was determined using the pH drift method [35]. Flasks containing 50 mL of a 0.01 $mol{\cdot}L^{-1}$ NaCl solution were first deoxygenated by N_2 bubbling for 2 h. The pHs of the deoxygenated solutions were then adjusted to successive initial values (pH_i) between 2 and 12, by addition of 0.1 $mol{\cdot}L^{-1}$ HCl or NaOH. 0.15 g of AC was introduced in the flasks which were maintained stoppered under agitation for 48 h, time after which final pH values (pH_f) were measured. The pH_{PZC} of a sample was determined graphically by the values for which pH_i was equal to pH_f.

"Boehm" titrations were performed to quantify the basic and oxygenated acidic surface groups on the ACs [36]. Carboxylic (R–COOH), lactonic (R–OCO), phenolic (Ar–OH) and basic groups were determined using different reactants, assuming that: NaOH reacted with the three acid groups, Na_2CO_3 did not react with Ar–OH groups and that $NaHCO_3$ only reacted with R–COOH groups. Basic groups' contents were determined using HCl. Typically, 0.15 g of each carbon sample was mixed with 50 mL of a 0.01 $mol{\cdot}L^{-1}$ aqueous reactant solution (NaOH or Na_2CO_3 or $NaHCO_3$ or HCl). The mixtures were stirred at a constant speed of 650 rpm at room temperature for 48 h. After that, the suspensions were filtered off through 0.45 µm membrane filters (Durapore®-Millipore). Back titrations of the filtrate (10 mL) were performed with standardized HCl or NaOH solutions (0.01 $mol{\cdot}L^{-1}$) in order to determine the oxygenated and basic groups' contents, respectively.

2.3.3. Textural characterization

The iodine number of the ACs was measured according to the ASTM D4607-94 (1999) standard.

To determine the methylene blue (MB) index ($mg{\cdot}g^{-1}$), 0.1 g of AC was poured in 25 mL of a 1.2 $g{\cdot}L^{-1}$ aqueous MB solution and maintained under stirring for 30 min. After filtration, the residual MB concentration was measured by UV-visible spectroscopy (at 665 nm) and the methylene blue index was calculated ($mg{\cdot}g^{-1}$).

MB was also used as probe molecule to sound the porosity of the ACs. The methylene blue surface area (SMB

in $m^2 \cdot g^{-1}$) was calculated from the adsorption isotherms according to the following formula [37].

$$SMB = (b \times Na \times S)/M_{MB}$$

where b is the maximum adsorption capacity ($g \cdot g^{-1}$), S is the surface occupied by one MB molecule (119×10^{-10} m^2), M_{MB} is the molecular weight of one MB molecule (319.86 $g \cdot mol^{-1}$) and Na is the Avogadro number.

N_2 adsorption–desorption isotherms (at 77K) and CO_2 adsorption isotherms (at 273K) of the ACs were measured using a Micromeritics ASAP 2020 sorptometer. Prior to the measurements, the samples were degassed under vacuum (10^{-5} mbar) at 250°C for 12 h. The specific surface areas (S_{BET}) were calculated in the [0.01–0.05] P/P° range, using the BET (Brunauer–Emmett–Teller) equation by assuming the area of the nitrogen molecule to be 0.162 nm^2 [38]. Pore size distributions (PSD) of the ACs were determined by using a "carbon finite slitpores" NLDFT (non-local density functional theory) model applied on the N_2 adsorption-desorption isotherms. Additionally, the ultramicroporous volumes (pores of diameters smaller than 0.7 nm) were evaluated by using a "carbon slit pores" NLDFT model applied on the CO_2 adsorption isotherms [39,40]

2.4. Methylene blue adsorption

Adsorption kinetics of methylene blue (MB) were studied at the initial concentration of 1600 $mg \cdot L^{-1}$ for the six prepared ACs (0.1 g of adsorbent in agitated flasks of 25 mL).

Aqueous solutions of methylene blue of initial concentration (C_i) ranging between 100 and 2000 $mg \cdot L^{-1}$ were prepared and used to study the MB adsorption isotherms of the six prepared ACs. A mass m of about 0.1 g of adsorbent was introduced in the MB solutions (V = 25 mL) and stirred for 2 h at room temperature, as it was determined from kinetics studies that equilibrium was reached after this contact time. The pH of the suspensions was adjusted by using NaOH solutions (1 $mol \cdot L^{-1}$) and measured at about pH 5. After filtration, the MB equilibrium concentrations (C_e) in solution were measured by UV-visible spectroscopy (λ = 665 nm). The MB uptake at equilibrium (Q_e, $mg \cdot L^{-1}$) was calculated from the relation: $Q_e = (C_e - C_i) \times V/m$.

3. Results and discussion

3.1. Biopolymer quantification

3.1.1. Thermogravimetric analysis (TGA)

TGA curves of the apricot and loquat stones exhibit three weight losses whereas only two have been observed on the curve of the date stones (Fig. 1). The first weight loss below 150°C, attributed to the elimination of physisorbed water, reaches about 7%, whatever the nature of the precursor. The second weight loss, starting at ~200°C and also observed for the three singly samples, can be attributed to the hemicellulose decomposition, with 14%, 36% and 65% in apricot, date and loquat stones, respectively (Fig. 1) [41]. This second weight loss is superimposed to a third one, starting at ~300°C and attributed to the decomposition of both cellulose and lignin biopolymers [41]. This third loss

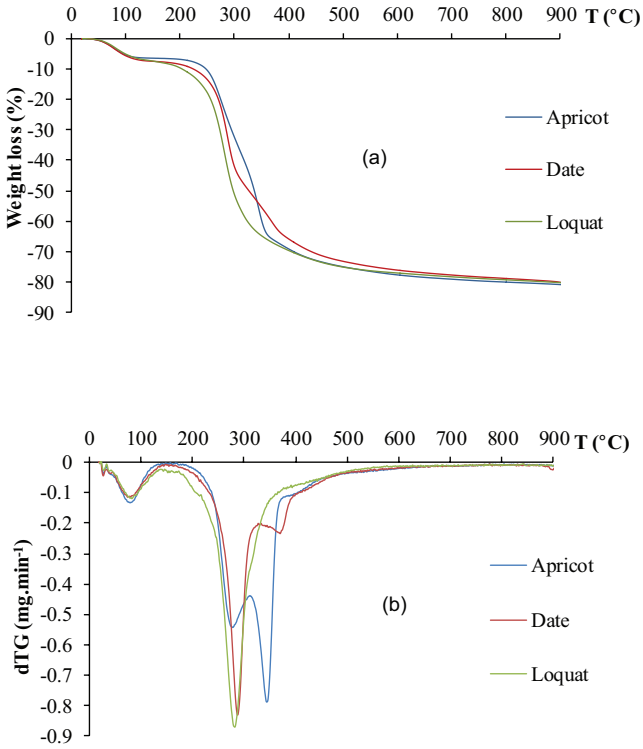

Fig. 1. TGA (a) and dTG (b) curves of the lignocellulosic precursors.

is the most important for apricot stones (~35%). Date stones contain about 16% of cellulose and lignin whereas loquat stones contain very few amounts of them as shown by the small shoulder at ~320°C observed on the dTG curve of this precursor (Fig. 1b). The amounts of cellulose and lignin cannot be determined accurately due to the overlapping of the TGA decomposition signals [42]. However, it can be clearly concluded from these curves that the three lignocellulosic precursors contain different proportions of the three biopolymers. Whereas loquat stones are quite exclusively composed of hemicellulose, date stones mainly contain hemicellulose and few amounts of cellulose and lignin, which are both the main constituents of apricot stones.

3.1.2. Biopolymer chemical analysis

The results of biopolymer content in each precursor (Table 1) show that the lowest content in lignin (8%) and cellulose (2%) have been obtained for the loquat stones which is also the softest material compared to apricot and date stones. The loquat stones are also the richest in hemicellulose (>50%) confirming the TGA results. The apricot stones display the highest content of cellulose (about 30%) compared to other precursors.

3.2. Elemental analysis

The elemental analyses of the ground stones have shown high carbon element content (~65% to 75%, Table 2), confirming that these biomaterials are interesting precur-

Table 1
Results of biopolymer and extractable organics contents in the lignocellulosic precursors

Stone origin	Extractable organics %	Lignin %	Cellulose %	Hemicellulose %
Apricot	8.4	18.1	31.1	39.1
Date	17.8	14.9	9.3	41.4
Loquat	16.1	8.2	2.5	50.3

Table 2
Results of the elemental analysis of the lignocellulosic precursors and the activated carbons produced there from

Sample	Element (mass%)				
	C	H	N	S	O
Apricot stones	75.3	9.3	0.73	0.01	14.6
Date stones	71.9	8.7	1.3	0.14	17.9
Loquat stones	65.0	9.3	1.5	0.07	24.2
A	85.6	1.3	0.74	–	12.3
D	86.3	1.3	1.7	–	10.7
L	85.1	1.7	1.8	–	11.4
A/L	75	2.1	1.3	–	21
A/D	65	1.8	0.8	–	24
D/L	68	1.9	1.1	–	19

sors for the preparation of ACs. They also contain oxygen (14–24%), hydrogen (~9%), and small amounts of nitrogen (<1.5%) and sulfur (<0.14%).

The carbon content of A, D and L AC samples was almost similar and of about 85%. An oxygen and hydrogen content decrease was measured concomitant to this carbon content increase. Whereas the nitrogen content was almost unchanged after activation, the sulfur content fell below the detection limit of the apparatus. The absence of this element can be explained by a decomposition of the sulfur in volatile sulfur oxides during the thermal treatment at 700°C.

The ash contents of the ACs vary between 0.1% and 3.7% (Table 2). The lowest value was obtained for the D activated carbon, which is consistent with its highest carbon content (i.e. 86.3% of C, Table 1). Among the ACs prepared from mixtures of precursors, those including date stones possess the lowest ash contents (1.8% and 2.1% for samples D/L and A/D, respectively). The highest ash content value was measured for A/L sample (3.7%, Table 1), and is in agreement with the ones of singly A and L samples (≥1%) indicating higher amounts of mineral species in apricot and loquat stones than in date ones. In any case, the determined ash content values (<1.2%) make the three lignocellulosic materials suitable for the preparation of ACs. Energy dispersive X-ray microanalysis (not shown) of the AC ashes confirmed the main presence of carbon (~80%) but also the presence of some metallic elements, namely Na, K, Mg, Ca, Fe, Cu, Zn, Al and Si. Traces of P and S originating from the precursors were also evidenced by X-ray microanalysis.

The yields of the ACs syntheses varied between 23% and 35% with associated weight losses ranging between ~65 and 77% (Table 3). The lowest yield was obtained for D sample, which was the one elaborated with the highest impregnation ratio (1.25). The results of Table 3 suggest that the burn-off globally increases together with the impregnation ratio confirming the key role of phosphoric acid in the activation mechanism.

Table 3
Ash content and burn-off of the ACs and corresponding phosphoric acid impregnation ratio

Activated carbon	Ash content (%)	Impregnation ratio	Burn-off (%)
A	1.0	1.20	67.2
D	0.1	1.25	76.7
L	1.2	0.80	73.9
A/L	3.7	0.65	65.0
A/D	2.1	1.00	68.4
D/L	1.8	0.40	69.7

3.3. Characterization of the surface chemistry of the activated carbons

3.3.1. Infrared spectroscopy

Infrared spectra of all six prepared ACs are very similar (Fig. 2) with the presence of characteristic signals of oxygenated surface groups.

The broad peak centered at 1170–1180 cm^{-1}, is attributed to C-O stretching in carboxylic acids, phenolic, ether, ester and lactonic groups [43]. The shoulder at 1050–1060 cm^{-1} which is a little more pronounced on the A/L spectrum can be assigned to the P-O stretching in phosphate groups [44] and to ionized linkage (P^+–O^-) in acid phosphate esters [8]. The attribution of this signal to phosphorous groups is strengthened by the phosphorous detection using EDS (not shown) and the chemical analyses (Table 2) revealing the highest ash content for A/L sample compared to the other ones. Peaks at 875 cm^{-1} were also observed confirming the presence of phosphorous compounds for activated carbons A/D and D/L (signature of P-OH). The bands at 960 cm^{-1} for A, D, L, and A/D are assigned to C-H aromatic links.

The single peak at about 1560 cm^{-1} can be assigned to C=O stretching vibrations of ketones, aldehydes [19] and to C=C stretching modes of aromatic rings [45].

The very low intensity peaks at ~2792 and 2868 cm^{-1} mainly observed on the spectra of D, L and A/L samples correspond to aliphatic C–H stretching vibration mode [19].

The broad signal in the 3000–3600 cm^{-1} range corresponds to the O-H stretching vibration mode of surface-adsorbed water molecules and to some hydrogen-bonded hydroxyl groups from carboxyls, phenols or alcohols.

3.3.2. pH_{PZC}

All the prepared ACs presented low pH_{PZC} values, varying between 2 and 4 in the same range than those measured

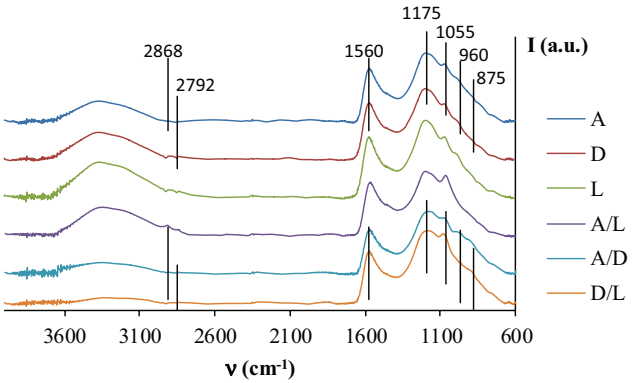

Fig. 2. Infrared spectra of the different activated carbons.

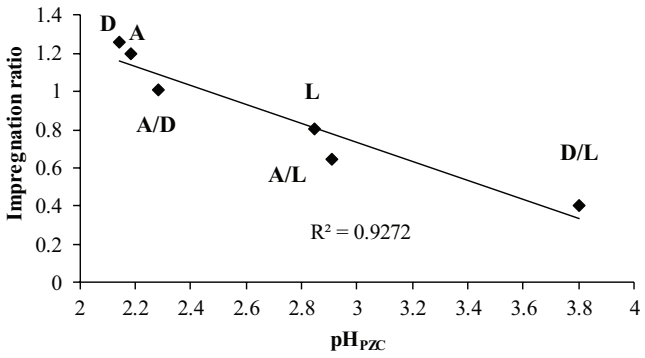

Fig. 3. Relation between the pH_{PZC} of the activated carbons and the phosphoric acid impregnation ratio.

by other authors after fruit stone phosphoric activation [29,46]. The measured pH_{PZC} values are consistent with the Boehm titration results (section 3.3.3.) showing a large predominance of acidic group. The plot of the impregnation ration versus pH_{PZC} clearly shows a linear correlation between both parameters (Fig. 3). The pH_{PZC} decreases as the impregnation ratio increases.

3.3.3. Boehm titration

The six ACs all possess significant amounts of carboxylic, lactonic and phenolic surface groups and small amounts of basic ones (Fig. 4). They are all mainly acidic as the number of basic surface groups is much lower than the total number of acid groups. These titration results are in good agreement with the pH_{PZC} values measured below 3.8 (Fig. 3). They are also consistent with the infrared spectroscopy analyses as carboxylic, lactonic and phenolic groups were identified through C-O, C=O and O-H vibration modes (Fig. 2).

The most acidic ACs have stemmed from date and apricot stones (pH_{PZC} ~ 2.2 for A and D ACs; pH_{PZC} ~ 2.0 for A/D sample). This high acidic character might be the consequence of the presence of high amounts of carboxylic groups, i.e., groups with the lowest pKa values (pKa-carboxylic ~ 4–5; pKa-lactonic ~ 8.2; pKa-phenolic ~ 10; pKa-carbonyl ~ 16–20). Compared to ACs prepared from apricot and/or date stones, the ACs derived from loquat stones possess lower amounts of carboxylic and lactonic groups and higher amounts of phenolic ones, conferring them a less acidic character (Figs. 3 and 4). The D/L sample prepared from a mixture of date and loquat stones possesses the highest amount of basic groups (Fig. 4, ~0.8 meq·g^{-1}) and lowest amount of carboxylic ones (Fig. 4, ~ 0.3 meq·g^{-1}) and consequently, the highest pH_{PZC} (Fig. 3, D/L sample, pH_{PZC} ~ 3.8).

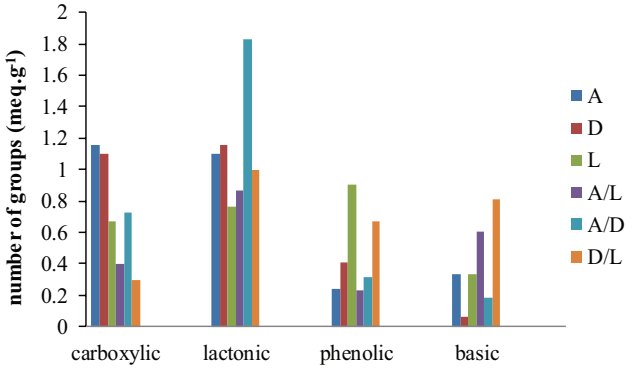

Fig. 4. Acid and basic functional groups determined by Boehm titration.

3.4. Textural properties of the activated carbons

3.4.1. Iodine number and methylene blue index

Iodine number and methylene blue index are closely linked to the BET surface area determined by N_2 adsorption and also to the porous volumes obtained from N_2 and CO_2 adsorption isotherms.

As expected, the iodine numbers of the precursors were rather low, as these biomaterials are not attended to be porous. The highest iodine number value of 293 mg·g^{-1} has been obtained for the apricot stone powder, compared to loquat and date stone ones (187 mg·g^{-1} and 11 mg·g^{-1}, respectively). This suggests that this biomaterial can favorably sorb iodine.

The phosphoric activation of the precursors has led to a significant increase in iodine number, highlighting the efficiency of the process to produce microporous adsorbents (Fig. 5). The iodine numbers of the six ACs varied between ~600 and 780 mg·g^{-1}. The highest value was obtained for the sample prepared from a mixture of apricot and loquat precursors. Samples L, A/D and D/L had similar iodine numbers which were among the lowest obtained values (~600 mg·g^{-1}).

The methylene blue indexes of all prepared ACs are of the same order of magnitude. Values vary between 253 mg·g^{-1} and 286 mg·g^{-1}, implying the presence of wide micropores and mesopores for all the six substrates. The ACs prepared from date or loquat stones, or from the mixture of both of them, possess the highest MB indexes (Fig. 5), indicating that date and loquat stones might be interesting precursors to elaborate mesoporous adsorbents. In a previous study, Mouni et al. prepared some ACs from apricot stones

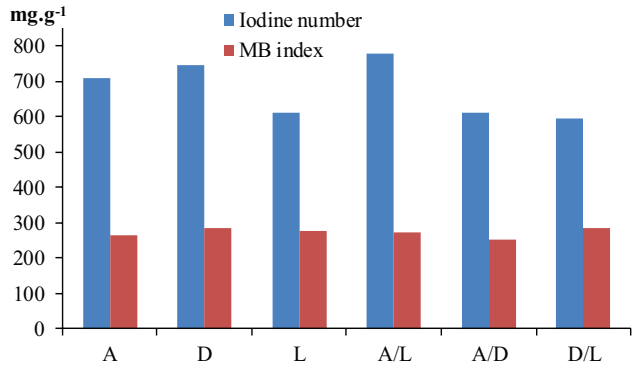

Fig. 5. Iodine number and methylene blue index (in mg·g^{-1}) of the activated carbons.

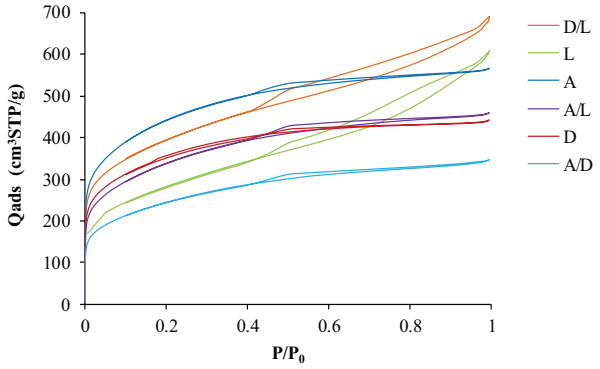

Fig. 6. N_2 adsorption-desorption isotherms (77 K) of the activated carbons.

[28] by H_2SO_4 (50%) activation at 200°C, followed by a carbonization at 650°C. The obtained AC was characterized by a low iodine number and a low methylene blue index (154 mg·g^{-1} and 91 mg·g^{-1}, respectively) and thus, a low BET surface area (393 m^2·g^{-1}) associated to a small porous volume (0.192 cm^3·g^{-1}). According to our measured iodine numbers and methylene blue indexes, higher surface areas with significant developed porosities are expected for our prepared ACs.

3.4.2. BET surface areas and pore size distributions

The N_2 adsorption-desorption isotherms of the ACs showed a type IV behavior with H4 hysteresis loops (Fig. 6), characteristic of mesoporous materials, with hydrophilic properties [47]. However, the hysteresis loops are more pronounced for L and D/L samples than for the other ACs. All samples present significant adsorption at low P/P° values (~455 to 680 cm^3·g^{-1}) which is characteristic of the presence of micropores. These isotherm shapes confirm the iodine number and MB index results previously discussed, suggesting that here-prepared ACs are both micro and mesoporous.

The determined BET specific surface areas (Table 4), ranging between 846 m^2·g^{-1} and 1495 m^2·g^{-1} (Table 4) are typical of ACs obtained by phosphoric activation of lignocellulosic precursors [48]. The ACs having the highest surface areas (sample A and D/L) also possess the highest microporous volumes (Table 3, 0.58 cm^3·g^{-1} and 0.49 cm^3·g^{-1}, respectively). On the contrary, sample A/D has the lowest surface area (816 m^2·g^{-1}) and also the lowest measured microporous volume (0.31 cm^3·g^{-1}). The surface areas were calculated in the 0.01–0.05 P/P_0 range, as usually performed for porous carbons having more micropores than mesopores. The microporous volumes determined from the PSDs are higher than the mesoporous ones for all the samples (Table 4). The super- and ultra-microporous volumes of all the activated samples are almost equal (Table 4), except for sample D/L for which the ultra-microporous volume represents about 40% of the total micro-porosity.

The highest mesoporous volumes have been obtained for L and D/L samples prepared from loquat stones (Table 4). They are of 0.65 cm^3·g^{-1} for the AC obtained from loquat exclusively and of 0.53 cm^3.g^{-1} for the one prepared from a mixture of loquat and date stones (sample D/L, Table 4). This result is in agreement with the largest hysteresis observed on the N_2 adsorption-desorption isotherms of these two samples (Fig. 6). The hysteresis observed on the curve of the sample A/L is narrower (V_{meso} = 0.24 cm^3·g^{-1}). This might be due to the presence of the apricot precursor which would have favored the formation of micropores rather than of mesopores. The pore size distributions (Fig. 7) also illustrate that L and D/L ACs possess larger mesopores in the whole 2–25 nm diameter range, contrary to the other samples having only small mesopores of diameter below ~7 nm. Moreover, L and D/L are the samples having the highest total porous volumes (Table 4, 1.02 cm^3·g^{-1}). The less porous samples are the ACs prepared from the date precursor, i.e., samples A/D and D, for which the total porous volumes are only of 0.51 cm^3·g^{-1} and 0.65 cm^3·g^{-1}, respectively (Table 4).

The ratio of mesopore volume to the micropore volume is known from literature to increase together with the impregnation ratio but in our study the samples prepared at the highest impregnation ratios (i.e. A and D prepared at about 1.2 impregnation ratio) are mainly

Table 4
Specific surface areas and porous volumes of the activated carbons. The porous volume occupied by methylene blue (V_{MB}) after its adsorption at saturation, is compared to the volume of pores in the diameter size range 1.3–2 nm ($V_{[1.3–2]\,nm}$) determined from the pore size distribution.

Activated carbon	A	D	L	A/D	A/L	D/L
S_{BET} (m^2·g^{-1})	1495	1204	1036	816	1128	1345
$V_{ultramicro}$ [a] (cm^3·g^{-1})	0.27	0.24	0.19	0.15	0.20	0.19
$V_{supermicro}$ [b] (cm^3·g^{-1})	0.31	0.23	0.16	0.16	0.23	0.30
V_{micro} [b] (cm^3·g^{-1})	0.58	0.47	0.35	0.31	0.43	0.49
V_{meso} [b] (cm^3·g^{-1})	0.25	0.18	0.67	0.20	0.24	0.53
V_{total} (cm^3·g^{-1})	0.83	0.65	1.02	0.51	0.68	1.02
V_{MB} (cm^3·g^{-1})	0.13	0.14	0.11	0.16	0.11	0.09
$V_{[1.3–2]\,nm}$ (cm^3·g^{-1})	0.22	0.16	0.16	0.12	0.17	0.18

[a]from N_2 adsorption, [b]from CO_2 adsorption.

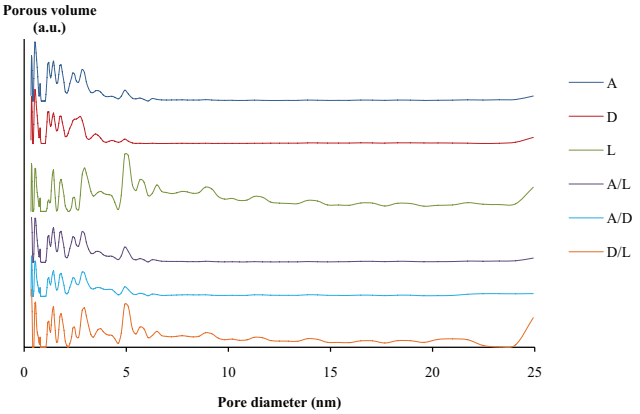

Fig. 7. Pore size distributions obtained from N_2 adsorption-desorption isotherms at 77 K (0.7 nm <ϕ_{pores}) and CO_2 adsorption isotherms at 273 K (ϕ_{pores} < 0.7 nm).

microporous while the samples prepared at the lower impregnation ratios (i.e. D/L and L prepared at 0.4 and 0.8 impregnation ratios, respectively) are mainly mesoporous. Thus, no clear correlation of the % of microporous volumes or the % of mesoporous volume (with respect to the total volume) as a function of the impregnation ratio was found.

The measured porosities can be correlated to the compositions of the precursors in biopolymers. Indeed, Guo et al. who studied ACs synthesized from xylan (i.e. hemicellulose), cellulose, and lignin by H_3PO_4 activation demonstrated that, for a given impregnation ratio, the microporous/mesoporous ratio depends on the nature of the precursor [25]. At impregnation ratio lower than 1.1, which are almost similar conditions as ours (impregnation ratio in the 0.4–1.25 range), they showed that hemicellulose favored the development of mesopores, while cellulose and lignin promoted the formation of micropores respectively. Similar trends were observed for our studied precursors as the most mesoporous ACs were obtained from loquat precursors (V_{meso} = 0.67 $cm^3 \cdot g^{-1}$) which are the ones containing the largest amounts of hemicellulose (Fig. 1, ~65%). Moreover, apricot precursors led to the ACs with larger amounts of micropores compared to the ones of mesopores (Table 4, V_{meso} = 0.25 $cm^3 \cdot g^{-1}$; V_{micro} = 0.58 $cm^3 \cdot g^{-1}$), in agreement with their high cellulose content (Fig. 1, ~ 35%). The plot of the ratio of hemicellulose percentage to the sum of cellulose and lignin percentages (% hemicellulose/(% cellulose+% lignin)) versus the mesoporous volume percentage (with respect to the total pore volume) for the prepared activated carbons is represented in Fig. 8. This plot confirms a correlation (R^2 = 0.8289) of the mesoporous volume percentage with the proportion of hemicellulose with respect to cellulose and lignin.

3.5. Methylene blue adsorption

Adsorption kinetics of methylene blue by the six prepared ACs (Fig. 9) show that equilibrium was reached after less than 2 h contact time, as previously reported for activated carbon powders of small size particles in which the diffusion of MB is very quick [49]. The adsorption kinetics were found

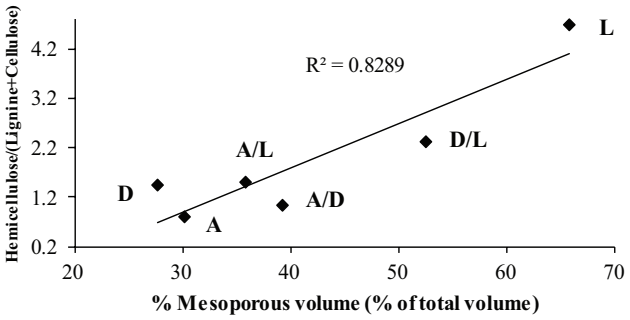

Fig. 8. Plot of the ratio of Hemicellulose/(Lignin+Cellulose) in the precursors as a function the activated carbons mesoporous volume (in % of the total volume of pore).

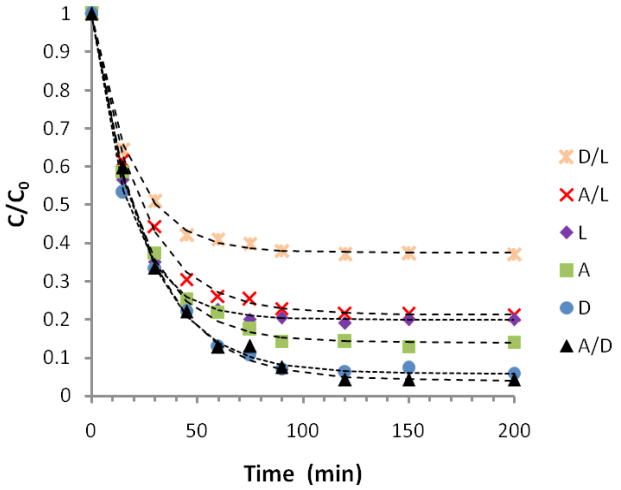

Fig. 9. Adsorption kinetics of methylene blue on the different prepared activated carbons. The dotted lines represent the fitted data using the pseudo first order model.

slightly quicker for the more mesoporous activated carbons (L and D/L) than for the microporous ones (D, A, A/L and A/D) and they were well fitted by pseudo first order law.

Adsorption isotherms of methylene blue by the six prepared ACs (Fig. 10) were well fitted by the Langmuir-Freundlich model (0.95 ≤ R^2 ≤ 0.99, RMSE ≤ 34).The Langmuir-Freundlich equation is $Q_e/Q_{max} = (K_{lf} \times C_e)^n/(1 + (K_{lf} \times C_e)^n)$ where Q_e is the adsorption uptake at equilibrium ($mmol \cdot g^{-1}$), C_e is the concentration at equilibrium ($mmol \cdot L^{-1}$), K_{lf} is the Langmuir-Freundlich constant ($L \cdot mmol^{-1}$), Q_{max} is the maximum uptake ($mmol \cdot g^{-1}$) and n is the Langmuir-Freundlich exponent. The Langmuir and Freundlich models were also tested but gave less satisfying results (R^2 ≤ 0.95). The maximum adsorption capacities ranged between ~250 $mg \cdot g^{-1}$ and ~440 $mg \cdot g^{-1}$ for the AC prepared from a mixture of date and loquat stones and the one prepared from a mixture of apricot and date stones, respectively (Table 5, samples D/L and A/D).

The determination of the microporous and mesoporous surfaces from N_2 adsorption-desorption isotherms suggests that the surface of all the adsorbents is mainly microporous (Table 5, S_{micro}/S_{meso} > 5.3), except for samples obtained from loquat stones (sample L, S_{micro}/S_{meso} ~ 2.3) and from a mix-

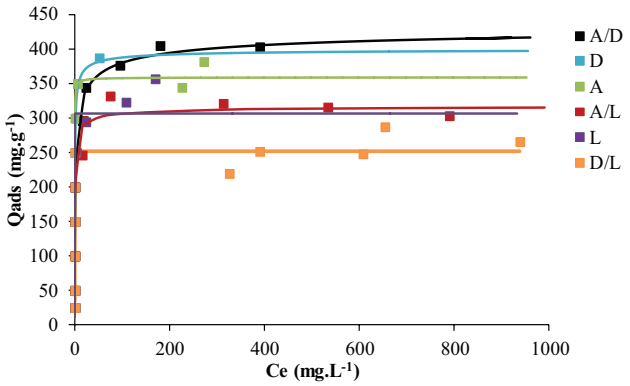

Fig. 10. Adsorption isotherms of methylene blue on the different prepared activated carbons.

ture of date and loquat stones (sample D/L, S_{micro}/S_{meso} ~ 0.6). As concluded from pore size distribution results, loquat stones appear to be responsible for the mesopore development. The surface occupied by the methylene blue molecule (calculated from Q_{max} and from the surface area of the molecule, see experimental part) is about one to eight times greater than the mesoporous surface for all the adsorbents (Table 5), which suggests that this molecule is adsorbed both on the mesoporous and microporous surfaces. The most efficient adsorbent for methylene blue is the AC prepared from a mixture of apricot and date stones (sample A/D), as confirmed by the maximum adsorption capacity of 443 $mg{\cdot}g^{-1}$ and also by the highest S_{MB}/S_{total} ratio of 1.26. This high ratio suggests either a multilayer adsorption or an adsorption on the external surface of the material. For the other five adsorbents, the S_{MB}/S_{total} ratio is lower than 1, indicating that the surface is not completely covered by the MB molecule. For all the microporous carbons (i. e. samples A, D and A/L), the MB coverage surface is lower than the microporous surface (Table 5), showing that MB molecules are possibly adsorbed in the micropores. For the L and D/L activated carbons, the MB coverage surface is higher than the microporous surface, showing that MB molecules are possibly adsorbed both in the micropores and mesopores.

An argumentation on the porosity occupied by adsorbed MB can be also based on the volume comparison. The volume occupied by adsorbed MB can be calculated from its molecular volume of 1.48 × 0.6 × 0.19 nm^3, estimated by Chemsketch, assuming a parallelepipedic molecule. The volume occupied by adsorbed MB can be compared to the volume of micropores having pore diameters in the range 1.3–2 nm, in agreement with our previous work showing the MB adsorption occurred in wide micropores [37] and the work of Graham [50] who mentioned a minimum pore size of 1.33 nm required for MB adsorption. Except for A/D activated carbon, the values of the pore volume of size ranging from 1.3 to 2 nm ($V_{[1.3\text{-}2]\,nm}$ reported in Table 4) are higher than the porous volume occupied by methylene blue (V_{MB}), demonstrating that MB might be accommodated in the wide micropores (namely supermicropores) in these activated carbons (samples A, D, L, A/L, and D/L).

The evolution of the maximum adsorption capacities (Fig. 10) and the pH_{PZC} values (Fig. 3) suggests that both parameters are closely linked. Indeed, the materials possessing the lowest pH_{PZC} values are the ones with the highest adsorption capacities (Fig. 11). This correlation indicates that the adsorption is favored by the electrostatic interactions between the negatively charged oxygen surface groups (particularly the carboxylate groups at the studied pH) of the AC and the positively charged methylene blue cation.

Table 5
Characteristic surface areas of the prepared ACs and coverage ratios of the surface accessible to methylene blue.

	A	D	L	A/D	A/L	D/L
Q_{max} ($mg{\cdot}g^{-1}$)	359	401	306	443	319	252
S_{MB} ($m^2{\cdot}g^{-1}$)	804	899	686	992	715	252
S_{total} ($m^2{\cdot}g^{-1}$)	1320	1176	856	787	957	968
S_{meso} ($m^2{\cdot}g^{-1}$)	157	123	258	118	152	227
S_{micro} ($m^2{\cdot}g^{-1}$)	1163	1053	598	669	805	140
S_{micro}/S_{meso}	7.4	8.6	2.3	5.7	5.3	0.6
S_{MB}/S_{total}	0.61	0.76	0.80	1.26	0.75	0.58

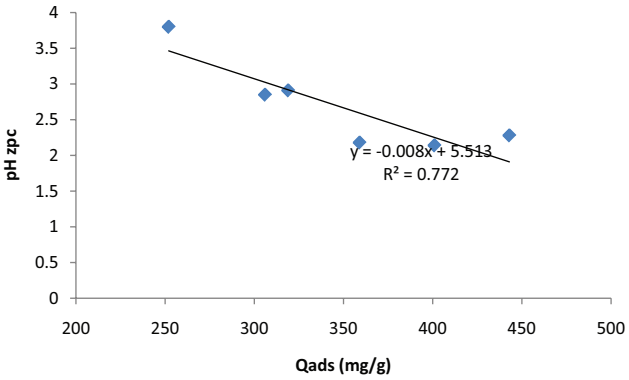

Fig. 11. Evolution of the methylene blue adsorption capacities versus pH_{PZC} values.

4. Conclusion

In this study, ACs of surface areas ranging between 816 and 1500 $m^2{\cdot}g^{-1}$ were prepared by chemical activation of apricot, loquat and date stones, stemming from the Algerian agro-food industry.

Physico-chemical characterization of the different obtained materials clearly suggests a correlation between the composition in biopolymer of the natural lignocellulosic precursor and the porosity size of the resulting AC made by phosphoric activation. It was found that the precursors having high hemicellulose contents, such as loquat stones have generated highly mesoporous ACs while the precursors richer in lignin and cellulose, such as apricot and date stones have generated mainly microporous ones. Thus, the preparation of binary mixtures of precursors in equal weight proportion and their further chemical activation by phosphoric acid, has allowed obtaining adsorbents with tailored porosities.

Due to their high porosity (porous volumes ranging between 0.51 $cm^3{\cdot}g^{-1}$ and 1.02 $cm^3{\cdot}g^{-1}$) and also to the presence

of high amounts of oxygenated surface groups (~1.5–3 meq·g^{-1}), the prepared adsorbents showed interesting properties towards the adsorption of methylene blue. Adsorption isotherms were well fitted by the Langmuir-Freundlich model (with $0.95 \leq R^2 \leq 0.99$, RMSE ≤ 34). The maximum adsorption capacities of this molecule, which is commonly used as reference to characterize an adsorbent, have been found in the 250–440 mg·g^{-1} range. Values of the same order of magnitude were typically obtained for ACs prepared by chemical activation of biomass of different origins [51]. Adsorption was favored by the acidity of the AC ($pH_{PZC} \leq 3.8$), which is also, as shown by Boehm titrations, governed by both the impregnation ratio and type of precursor. The coverage ratios of the ACs' surfaces by methylene blue were between 0.61 and 1.26. It was evidenced by the N_2 adsorption-desorption isotherms and the methylene blue adsorption isotherms that the dye cation was mainly adsorbed in the wide micropores and partially in the mesopores. A multilayer adsorption or an adsorption on the external surface was also suggested for the strongly acidic AC prepared from a mixture of apricot and date stones.

As agro-food industry generates large quantities of biomass, of varying composition in biopolymers, it might be of great interest to valorize these wastes by elaborating controlled porosity adsorbents of high adsorption capacities. In future prospects, the variation of the biopolymer composition in a mixture of precursors, i.e., the ratio of the precursors rich in hemicellulose (for example loquat) to the ones rich in lignin and cellulose could allow to prepare a series of ACs with a controlled microporosity/mesoporosity proportion at a given impregnation ratio.

Acknowledgments

The authors are grateful to the Algerian Higher Education and Scientific Research Ministry for financing the grant of Karima Larbi through the national project PNE 2016/2018.

References

[1] T. Thompson, M. Sobsey, J. Bartram, Providing clean water, keeping water clean, an integrated approach, Int. J. Environ. Health. Res., 13 (2003) 89–94.
[2] I. Ali, V.K. Gupta, Advances in water treatment by adsorption technology, Nat. Protoc., 1 (2006) 2661–2667.
[3] S.D. Faust, O.M. Aly, Adsorption processes for water treatment, first ed., Butterworth, Stoneham MA, 1987.
[4] M. Sanchez-Polo, J. Rivera-Utrilla, Adsorbent-adsorbate interactions in the adsorption of Cd (II) and Hg (II) on ozonized activated carbons, Environ. Sci. Technol., 36 (2002) 3850–3854.
[5] R. Radhika, T. Ayalatha, S. Acob, R. Rajeev, B.K. George, B.R. Anjali, Removal of perchlorate from drinking water using granular activated carbon modified by acidic functional group: Adsorption kinetics and equilibrium studies, Process Safety Environ. Protect., 109 (2017) 158–171.
[6] C.Y. Yin, M.K. Aroua, W.M.A.W. Daud, Review of modifications of activated carbon for enhancing contaminant uptakes from aqueous solutions, Sep. Purif. Technol., 52 (2007) 403–415.
[7] H. Marsh, F. Rodríguez Reinoso, Activated carbon, first ed., Elsevier, Oxford, 2006.
[8] A.M. Puziy, O.I. Poddubnayaa, A. Martınez-Alonso, F. Suarez-Garcıa, J.M.D. Tascon, Synthetic carbons activated with phosphoric acid I. Surface chemistry and ion binding properties, Carbon, 40 (2002) 1493–1505.
[9] M.A.A. Zaini, Y. Amano, M. Machida, Adsorption of heavy metals onto activated carbons derived from polyacrylonitrile fiber, J. Hazard. Mater., 180 (2010) 552–560.
[10] X. Zhao, S. Lai, H. Liu, L. Gao, Preparation and characterization of activated carbon foam from phenolic resin, J. Environ. Sci., 21 (2009) 121–123.
[11] J. Wang, T.L. Liu, Q.X. Huang, Z.Y. Ma, Y. Chi, J.H. Yan, Production and characterization of high quality activated carbon from oily sludge, Fuel. Process. Technol., 162 (2017) 13–19.
[12] M.A.P. Cechinel, A.A.U. Ulson de Souza, A.A. Ulson de Souza, Study of lead (II) adsorption onto activated carbon originating from cow bone, J. Clean. Prod., 65 (2014) 342–349.
[13] H. Benaddi, T.J. Bandosz, J.A. Jagiello, J.A. Schwarz, J.N. Rouzaud, D. Legras, F. Béguin, Surface functionality and porosity of activated carbons obtained from chemical activation of wood, Carbon, 38 (2000) 669–674.
[14] H. Deng, G. Zhang, X. Xu, G. Tao, J. Dai, Optimization of preparation of activated carbon from cotton stalk by microwave assisted phosphoric acid-chemical activation, J. Hazard. Mater., 182 (2010) 217–224.
[15] V. Gomez-Serrano, E.M. Cuerda-Correa, M.C. Fernandez-Gonzalez, M.F. Alexandre-Franco, A. Macıas-Garcıa, Preparation of activated carbons from chestnut wood by phosphoric acid-chemical activation, Study of microporosity and fractal dimension, Mater. Lett., 59 (2005) 846–853.
[16] V. Fierro, V. Torne-Fernandez, A. Celzard, Kraft lignin as a precursor for microporous activated carbons prepared by impregnation with ortho-phosphoric acid: Synthesis and textural characterization, Micropor. Mesopor. Mater., 92 (2006) 243–250.
[17] I.A.W. Tan, J.C. Chan, B.H. Hameed, L.L.P. Lim, Adsorption behavior of cadmium ions onto phosphoric acid-impregnated microwave-induced mesoporous activated carbon, J. Water Process. Eng., 14 (2016) 60–70.
[18] M. Molina-Sabio, F. Rodrıguez-Reinoso, Role of chemical activation in the development of carbon porosity, Colloids Surf. A Physicochem. Eng. Asp., 241 (2004) 15–25.
[19] A. Reffas, V. Bernardet, B. David, L. Reinert, M.B. Lehocine, L. Duclaux, Carbons prepared from coffee grounds by H_3PO_4 activation: Characterization and adsorption of methylene blue and Nylosan Red N-2RBL, J. Hazard. Mater., 175 (2010) 779–788.
[20] M. Kwiatkowski, D. Kalderis, E. Diamadopoulos, Numerical analysis of the influence of the impregnation ratio on the microporous structure formation of activated carbons, prepared by chemical activation of waste biomass with phosphoric (V) acid, J. Phys. Chem. Solids, 105 (2017) 81–85.
[21] B. Tiryaki, E. Yagmur, A. Banford, Z. Aktas, Comparison of activated carbon produced from natural biomass and equivalent chemical compositions, J. Anal. Appl. Pyrolysis, 105 (2014) 276–283.
[22] J. Deng, T. Xiong, H. Wang, A. Zheng, Y. Wang, Effects of cellulose, hemicellulose, and lignin on the structure and morphology of porous carbons, ACS Sustain. Chem. Eng., 4 (2016) 3750–3756.
[23] C. Rodriguez, C. Thomas Otto, A. Kruse, Influence of the biomass components on the pore formation of activated carbon, Biomass Bioenergy, 97 (2017) 53–64.
[24] M. Jagtoyen, F. Derbyshire, Activated carbons from yellow poplar and white oak by H_3PO_4 activation, Carbon, 36 (1998) 1085–1097.
[25] Y. Guo, D.A. Rockstraw, Physical and chemical properties of carbons synthesized from xylan, cellulose and Kraft lignin by H_3PO_4 activation, Carbon, 44 (2006) 1464–1475.
[26] O. Ioannidou, A. Zabaniotou, Agricultural residues as precursors for activated carbon production, Renew. Sustain. Energy Rev., 11 (2007) 1966–2005.
[27] J.M. Dias, M.C. Alvim-Ferraz, M.F. Almeida, J. Rivera-Utrilla, M. Sánchez-Polo,Waste materials for activated carbon preparation and its use in aqueous-phase treatment, J. Environ. Manage., 85 (2007) 833–846.
[28] L. Mouni, D. Merabet, A. Bouzaza, L. Belkhiri, Adsorption of Pb(II) from aqueous solutions using activated carbon developed from apricot stone, Desalination, 276 (2011) 148–153.

[29] M.H. Marzbali, M. Esmaieli, H. Abolghasemi, M.H. Marzbali, Tetracycline adsorption by H_3PO_4 activated carbon produced from apricot nut shells: A batch study, Process Safety Environ. Protect., 102 (2016) 700–709.
[30] Ç. Şentorun-Shalaby, M.G. Uçak-Astarlıoglu, L. Artok, Ç. Sarıcı, Preparation and characterization of activated carbons by one-step steam pyrolysis/activation from apricot stones, Micropor. Mesopor. Mater., 88 (2006) 126–134.
[31] M.L. Sekirifa, M. Hadj-Mahammed, S. Pallier, L. Baameur, D. Richard, A.H. Al-Dujaili, Preparation and characterization of an activated carbon from a date stones variety by physical activation with carbon dioxide, J. Anal. Appl. Pyrolysis, 99 (2013) 155–160.
[32] H. Sütcü, H. Demiral, Production of granular activated carbons from loquat stones by chemical activation, J. Anal. Appl. Pyrolysis, 84 (2009) 47–52.
[33] M. Plaza-Recobert, G. Trautwein, M. Pérez-Cadenas, J. Alcañiz-Monge, Superactivated carbons by CO_2 activation of loquat stones, Fuel Process. Technol., 159 (2017) 345–352.
[34] V.V. Do Thi, Matériaux composites fibres naturelles /polymère biodégradable, Ph. D Thesis, University of Grenoble, France, 2011.
[35] M.V. Lopez-Ramon, F. Stoeckli, C. Moreno-Castilla, F. Carrasco-Marin, On the characterization of acidic and basic surface sites on carbons by various techniques, Carbon, 37 (1999) 1215–1221.
[36] H.P. Boehm, Surface oxides on carbon and their analysis, a critical assessment, Carbon, 40 (2002) 145–149.
[37] M. Benadjemia, L. Millière, L. Reinert, N. Benderdouche, L. Duclaux, Preparation, characterization and Methylene Blue adsorption of phosphoric acid activated carbons from globe artichoke leaves, Fuel. Process. Tech., 92 (2011) 1203–1212.
[38] K. Kaneko, C. Ishii, Super high surface area determination of microporous solids, Colloids Surf., 67 (1992) 203–212.
[39] J. Jagiello, M. Thommes, Comparison of DFT characterization methods based on N_2, Ar, CO_2, and H_2 adsorption applied to carbons with various pore size distributions, Carbon, 42 (2004) 1227–1232.
[40] J. Jagiello, J.P. Olivier, A simple two dimensional NLDFT model of gas adsorption in finite carbon pores, Application to pore structure analysis, J. Phys. Chem. C., 113 (2009) 19382–19385.
[41] J. Yu, N. Paterson, J. Blamey, M. Millan, Cellulose, xylan and lignin interactions during pyrolysis of lignocellulosic biomass, Fuel, 191 (2017) 140–149.
[42] H. Zhou, Y. Long, A. Meng, Q. Li, Y. Zhang, The pyrolysis simulation of five biomass species by hemi-cellulose, cellulose and lignin based on thermogravimetric curves, Thermochim. Acta, 566 (2013) 36–43.
[43] S.J. Park, B.J. Park, S.K. Ryu, Electrochemical treatment on activated carbon fibers for increasing the amount and rate of Cr (VI) adsorption, Carbon, 37 (1999) 1223–1226.
[44] S. Bourbigot, M. Le Bras, R. Delobel, Carbonization mechanisms resulting from intumescence. II. Association with an ethylene terpolymer and the ammonium polyphosphate-pentaerythritol fire retardant system, Carbon, 33 (1995) 283–294.
[45] E. Sabio, E. Gonzalez, J.F. Gonzalez, C.M. Gonzalez-Garcia, A. Ramiro, J. Ganan, Thermal regeneration of activated carbon saturated with p-nitrophenol, Carbon, 42 (2004) 2285–2293.
[46] M. Olivares-Marín, C. Fernández-González, A. Macías-García, V. Gómez-Serrano, Porous structure of activated carbon prepared from cherry stones by chemical activation with phosphoric acid, Energy Fuels, 21 (2007) 2942–2949.
[47] J. Rouquerol, F. Rouquerol, P. Llewellyn, G. Maurin, K.S.W. Sing, Adsorption by powders and porous solids: principles, methodology and applications, second ed., Academic Press, Oxford, 2014.
[48] A.M. Youssef, N.R.E. Radwan, I. Abdel-Gawad, G.A.A. Singer, Textural properties of activated carbons from apricot stones, Colloids Surf. A Physicochem. Eng. Asp., 252 (2005) 143–151.
[49] S. Agarwal, I. Tyagi, V.K. Gupta, N. Ghasemi, M. Shahivand, M. Ghasemi, Kinetics, equilibrium studies and thermodynamics of methylene blue adsorption on Ephedra strobilacea saw dust and modified using phosphoric acid and zinc chloride, J. Mol. Liq., 218 (2016) 208–218.
[50] D. Graham, Characterization of physical adsorption systems III, The separate effects of pore size and surface acidity upon the adsorbent capacities of activated carbons, J. Phys. Chem., 59 (1955) 896–900.
[51] E. Altintig, H. Altundag, M. Tuzen, M. Sari, Effective removal of methylene blue from aqueous solutions using magnetic loaded activated carbon as novel adsorbent, Chem. Eng. Res. Design, 122 (2017) 151–163.